Journal of Maps

Taylor & Francis
Taylor & Francis Group

ISSN: (Print) (Online) Journal homepage: https://www.tandfonline.com/loi/tjom20

Geology of the Montigiu Nieddu metamorphic basement, NE Sardinia (Italy)

Gabriele Cruciani , Marcello Franceschelli , Giovanni Musumeci & Massimo Scodina

JOURNAL OF MAPS
2020, VOL. 16, NO. 2, 543–551
https://doi.org/10.1080/17445647.2020.1785344

Science

OPEN ACCESS Check for updates

Geology of the Montigiu Nieddu metamorphic basement, NE Sardinia (Italy)

Gabriele Cruciani[a], Marcello Franceschelli[a], Giovanni Musumeci[b] and Massimo Scodina[a]

[a]Dipartimento di Scienze Chimiche e Geologiche, Università degli Studi di Cagliari, Cagliari, Italy; [b]Dipartimento di Scienze della Terra, Università di Pisa, Pisa, Italy

ABSTRACT
A geological map at 1:10,000 scale is presented that shows the distribution of the metamorphic rock units in the area of Montigiu (Mt.) Nieddu (NE Sardinia). These units belong to the High-Grade Metamorphic Complex in the Inner Zone of the Variscan chain of Sardinia. The rocks include different types of migmatite, amphibolite, and retrogressed eclogites. The geological map and cross section show the complex tectonic and metamorphic setting of the area, whereas the metamorphic assemblages and deformation framework represent a valuable tool for the reconstruction of the P-T metamorphic evolution for the crustal sectors involved in the Variscan orogeny. The metamorphic rock units reported in the map derived from the lower and upper continental plates involved in the Variscan collision and were tectonically juxtaposed during the early Carboniferous exhumation stage.

ARTICLE HISTORY
Received 22 April 2020
Revised 16 June 2020
Accepted 17 June 2020

KEYWORDS
Migmatite Complex; amphibolite; metamorphic units; P-T evolution; Variscan Sardinia

1. Introduction

The Sardinian Variscan belt has been subdivided into three main tectono-metamorphic zones from SW to NE: External Zone, Nappe Zone, and Inner Zone (Carmignani et al., 2001). The Inner Zone, which also extends to southern Corsica (Massonne et al., 2018), is subdivided into a southern Low to Medium-Grade Metamorphic Complex (L-MGMC) and a northern High-Grade Metamorphic Complex (HGMC, or Migmatite Complex), separated by the Posada-Asinara tectonic line, a km-wide NW – SE trending shear zone (Carmignani et al., 1994, 2001).

In this paper we present a detailed geological map (Main Map) of high-grade metamorphic rocks exposed in an area of ca. 7–8 km^2 north of Olbia, comprising the Montigiu (Mt.) Nieddu, Nodu Pianu, Sos Aranzos and Iles localities. This area, characterized by the occurrence of gneisses, high-pressure (HP) migmatites and metabasites with eclogite and granulite facies relics, is of significant relevance for the dynamics of the Variscan continent-continent collision.

2. Geological setting

The Migmatite Complex in the Inner Zone consists of HP migmatite and paragneiss with polyphase deformation (Cruciani et al., 2014a, 2014b; Fancello et al., 2018; Massonne et al., 2013) and sillimanite + K-feldspar metamorphic grade (Franceschelli et al., 2005). Orthogneisses, calc-silicate nodules and metabasite with eclogite and granulite facies relics also occur (Cruciani et al., 2011, 2012, 2015a, 2015b; Franceschelli et al., 2007). In the Golfo Aranci area (5–6 km NE of the mapped area), Elter et al. (2010) further subdivide the HGMC into two amphibolite facies: the Old Gneiss Complex and New Gneiss Complex.

A polyphase ductile deformation was recognized and described by several authors (Carosi et al., 2005; Cruciani et al., 2015c; Elter et al., 2010; Franceschelli et al., 2005). The early syn-collisional deformation phase (D1; Carmignani et al., 1994), is well preserved in the L-MGMC (Cruciani et al., 2013a, 2013b). Within the Migmatite Complex, D1 deformation is only documented by the transposition of centimetre-thick leucosomes. The D2 deformation phase is related to the development of NE-verging folds and dextral shear zones (e.g. Posada-Asinara line, Carosi et al., 2012 and references therein). In the migmatites the D2 phase is evidenced by WNW-ESE striking foliation (S2) and N140°-striking isoclinal folds gently plunging (5–20°) toward SE. Corsi and Elter (2006) documented the occurrence of two opposite senses of shear (top to NW and top to SE/NE) on the S1 and S2 foliation, respectively, related to D1 and D2 non-coaxial deformations. These authors associated the top-to-NW shearing with the end of compression and crustal thickening, whereas the top-to-SE/NE to tectonic inversion during the exhumation of the metamorphic basement. The D3 phase consists of upright metric to decametric open folds associated with an S3 axial-plane crenulation cleavage. The D4 phase is revealed by metric to decametric folds with sub-horizontal axial planes (Cruciani et al., 2015c). An overall

CONTACT Gabriele Cruciani gcrucian@unica.it Dipartimento di Scienze Chimiche e Geologiche, Università degli Studi di Cagliari, S.S. 554 Cittadella Universitaria, Monserrato (CA), 09042, Italy

description of the Variscan metamorphism and deformation can be found in Cruciani et al. (2015c). Intrusive rocks of the Sardinia-Corsica batholith are widely distributed in the Inner Zone of Variscan Sardinia (Casini et al., 2015 and references).

3. Methods

The Main Map at 1:10,000 scale covers an area of about 7–8 km^2 included in the municipal territories of Olbia and Golfo Aranci. The mapping was based on the original 1:10,000 vector topographic maps from 'Regione Autonoma della Sardegna – Carta Tecnica Regionale', Sections 44030 and 44040, called 'Cabu Abbas' and 'Golfo Aranci', respectively. Field data were localized by GPS and reported on the georeferenced digital map. The coordinate system is Monte Mario Ovest, projection Gauss-Boaga.

4. Lithostratigraphy

The study area (Figure 1 and Main Map) is located between the localities of Mt. Nieddu, Nodu Pianu, Sos Aranzos and Iles (NE of Olbia). It is featured by the occurrence of two metabasite lenses in Mt. Nieddu and Iles localities, hosted in the migmatite and gneiss of the HGMC.

The lithological sequence in Figure 1 and in the Main Map is based on field observations and geochronological data published by different authors (Cruciani et al., 2008a, 2008b; Ghezzo et al., 1979; Giacomini et al., 2005, 2006; Padovano et al., 2012, 2014). We have distinguished a Migmatite Unit, a Montigiu Nieddu Unit and an Eclogite Unit (Figure 1). The lithologies cropping out in the study area and represented in the Main Map will be described below:

4.1. Granites, pegmatites, leucocratic bodies

All metamorphic rocks in the study area are crosscut by granitic, pegmatitic and, less frequently, basic dykes. Pegmatitic dykes show a coarse-grained size, with quartz-feldspathic crystals up to 10 cm in size and millimetric to centimetric tourmaline crystals. The granitic rocks differ from the pegmatites for a yellowish colour and a finer grain size. Rare basic dykes, up to 1 m in width, are massive rocks with a general NNE-SSW direction.

Foliated leucocratic bodies with abundant coarse-grained muscovite and sub-millimetric garnet crystals are frequently observed within the migmatites and paragneiss (Figure 2(a)), mainly near to Punta Bados. These leucocratic bodies often occur as metric to decametric lenses of coarse- to medium-grained rocks with sharp contact to the host rock. At the interface between leucocratic bodies and the host migmatite or gneiss, folding and deformation involving the two lithologies are locally observed.

4.2. Migmatite Unit

In the Migmatite Unit the following main lithologies were distinguished:

4.2.1. Migmatite and gneiss

They are the dominant lithologies in the study area. Migmatites consist of coarse-grained whitish leucosomes, locally pegmatoid, parallel to or folded by the S2 schistosity and of darker medium-grained melanosomes. The migmatites show the typical layered structure locally strongly deformed with development of folds and boudins (Figure 2(b)). The migmatites contain centimetre-thick stromatic leucosomes which are mainly trondhjemitic (<1% modal K-feldspar) and, rarely, granitic in composition (Cruciani et al., 2008a). The rare granitic leucosomes differ from trondhjemitic ones for modal content of K-feldspar, which is up to 25% vol.%.

Paragneisses mostly occur at Bados peninsula and Nodu Pianu (Figure 1) and as small bodies elsewhere within the migmatites. The gneisses are brownish, fine-grained and with millimetric fibrolite nodules close to the contact with orthogneisses (Figure 2(c)). U/Pb dating on zircon suggests, for the migmatite protolith, a maximum deposition age of 480–450 Ma (Giacomini et al., 2006).

4.2.2. Amphibole-bearing migmatite

The amphibole-bearing migmatite forms a lens-shaped body (100–150 m in length and 50–70 m in width) in the southern part of the study area, close to Villaggio Bados (see Main Map). This rock shows a N 145° striking and steeply dipping foliation transposing leucosomes and quartz-feldspathic 'rods' (Cruciani et al., 2008b). The evidence of a pre-D2 deformation is the occurrence of a gneissose layering (D1) pre-dating the D2 folding phase. The amphibole-bearing migmatites display a discontinuous banding with alternation of quartz-feldspathic leucosomes and well-foliated biotite-bearing melanosomes (Figure 2(d)). Coarse-grained and weakly foliated leucosomes are parallel to the main schistosity, or folded. Coarse-grained amphibole grains up to 2 cm long are common in the leucosomes (Figure 2(d)). The contact between leucosome and melanosome is often marked by biotite-rich selvedges. The melanosome is characterized by a medium-grained size and a dark colour due to the abundance of biotite and amphibole, which are aligned to the foliation. The emplacement age of igneous protolith was constrained at 461 ± 12 Ma by a Pb-Pb isochron (Cruciani et al., 2008b).

4.2.3. Migmatized orthogneiss

Migmatized orthogneiss (and orthogneiss s.s.) occurs close to Punta Bados and Nodu Pianu as some

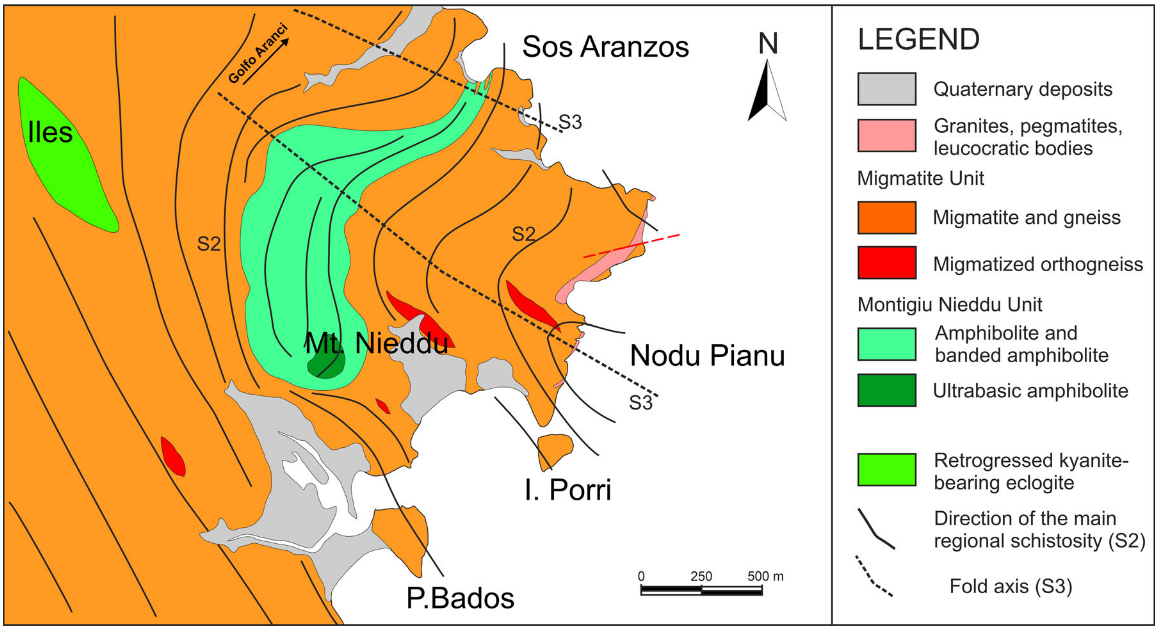

Figure 1. Geological sketch map of the Montigiu Nieddu metamorphic units.

metre- to decametre-thick lenticular bodies with NW-SE direction within the migmatites. Orthogneisses are greyish in colour, medium- to coarse-grained and show a pervasive foliation marked by the orientation of biotite crystals. Leucosomes are coarse-grained and centimetric in width. The boundary leucosome-melanosome is sharp and marked by biotite-rich selvedges, which, when folded, become thicker in the fold hinge. Melanosomes display a medium grain size and a dark colour due to the presence of abundant mafic minerals.

Locally, millimetric to centimetric garnet crystals occur. Orthogneiss, cropping out at Golfo Aranci dated by U/Pb zircon geochronology, yielded a Middle Ordovician emplacement ages of 469 ± 3.7 Ma (Giacomini et al., 2006).

4.3. Montigiu Nieddu Unit

The Mt. Nieddu Unit is a wide (2 km × 300–350 m) metabasite lens-shaped body oriented NE/SW to N/S. Two different lithologies can be distinguished: amphibolite and banded amphibolite, ultrabasic amphibolite.

4.3.1. Amphibolite and banded amphibolite

Amphibolite and banded amphibolite crop out as a large lens-shaped body, in which poorly foliated or massive rocks mainly occur in the core of the lens and well-foliated ones along the edge close to the host migmatite. The massive portions are slightly lighter in colour, related to a higher modal abundance of plagioclase. These rocks show a banded (flaky) structure with an alternation of centimetric to decimetric dark green, amphibole-rich bands and white, plagioclase-rich bands frequently folded and stretched along the S2. The amphibolites are featured by S2 parallel, white to greenish millimetric to centimetric epidote-rich veins and, locally, by centimetre-thick layers containing garnet porphyroblasts up to 1 cm in size (Figure 2(e)). The matrix of these layers mainly consists of amphibole and fine-grained symplectite-type microstructure.

The tectonic contact with the surrounding migmatites is slightly discordant with the S2.

4.3.2. Ultrabasic amphibolite

Ultrabasic amphibolites occur in a small lenticular body (about 100 m in length and 40–50 m in width) hosted within the banded amphibolite.

The ultrabasic amphibolite (i.e. the ultramafic amphibolites of Ghezzo et al., 1979) is an heterogeneous group of rocks characterized by the occurrence of relics of igneous minerals (pyroxene, olivine and plagioclase) and metamorphic minerals in variable amounts. These rocks are dark-coloured, characterized by a massive to poorly foliated texture and show a medium- to coarse-grained size. On the basis of mineral distribution and microstructures, three main compositional layers (A, B, C) have been distinguished (Franceschelli et al., 2002).

Layer A is 20 m thick and is featured by the occurrence of igneous olivine grains, locally rimmed by a discontinuous thin layer of orthopyroxene. Layer A shows a dark-grey colour with reddish shades, related to olivine oxidation. Amphibole and chlorite are also abundant.

The **Layer B** is about 5 m thick, lenticular in shape, dark grey to greenish in colour and mainly consists of greenish amphibole and large (up to 1 cm) plagioclase crystals. This layer is characterized by the occurrence of multilayer corona textures

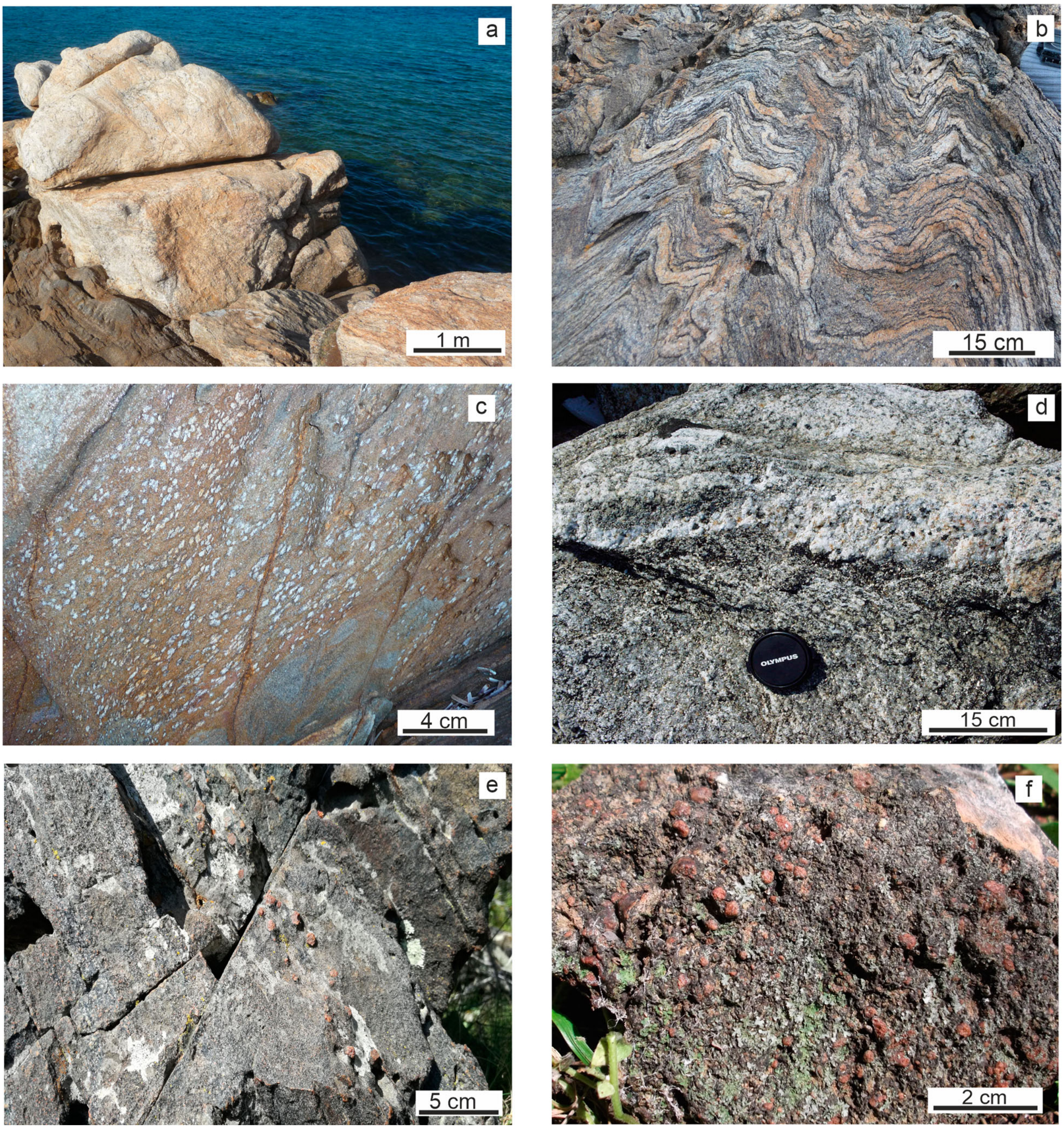

Figure 2. Field aspect of the main lithologies cropping out in the mapped area. (a) Punta Bados, leucocratic body crosscutting the paragneiss (bottom left corner); (b) folded leucosomes, parallel to the S2 schistosity, in the layered migmatite; (c) Paragneiss with oriented fibrolite nodules; (d) amphibole-bearing migmatite with centimetric amphibole crystals in the leucosome; (e) Garnet-rich layer in the banded amphibolite; (f) Iles locality, retrogressed eclogite with garnet porphyroblasts.

around igneous relics of olivine and plagioclase. These textures are characterized by orthopyroxene and/or clinopyroxene layers around olivine, and by garnet coronae and clinopyroxene + spinel symplectite surrounding plagioclase; all these minerals were overgrown by amphibole.

Layer C is about 15–20 m thick with a dark-green to reddish colour, due to the abundance of amphibole and garnet (the latter being up to 60–70%). This layer, occurring at the top of Mt. Nieddu, is characterized by millimetric porphyroblastic garnet and large amphibole grains up to 4–5 cm. Spinel, plagioclase, pyroxene, and chlorite also occur. Garnet-rich nodules, ranging in size from 1 to 15 cm, and garnet-, amphibole- and/or epidote-rich veins are also found.

4.4. Retrogressed kyanite-bearing eclogite

Massive to weakly foliated lens-shaped bodies of retrogressed eclogites show an alternation of garnet-rich and garnet-poor layers parallel to S2. They are dark-green in colour and fine- to medium-grained with millimetre- to centimetre-sized (1–2 cm) reddish garnet porphyroblasts and white pods of pyroxene + plagioclase symplectite (Figure 2(f)). Millimetre-sized, bluish kyanite crystals are less common but are the only example of kyanite among the Sardinian eclogites (Cruciani et al., 2019a). The dark-coloured matrix is mainly made up of green amphibole. The eclogite-facies minerals (i.e. garnet and omphacite) are best preserved in the garnet-rich layers, whereas in the garnet-poor layers the texture is dominated by clinopyroxene–plagioclase symplectite testifying a more pervasive retrograde overprint. Magmatic zircons from the Golfo Aranci eclogites, dated by the U–Pb method, yielded an Ordovician protolith age of 460 ± 5 Ma (Giacomini et al., 2005).

5. Tectonic and metamorphic evolution

5.1. Deformation

The described metamorphic rock units experienced a Variscan polyphase tectonic and metamorphic evolution. Deformation shows an heterogeneous distribution at the map and outcrop scale, mainly controlled by the difference in competence between rock types.

A relict D1 deformation is locally recognizable in (i) sigmoidal-shaped gneissic pods, (ii) quartzitic enclaves in migmatites and (iii) foliation in the paragneisses at Punta Bados.

The D2 phase, in all rock units, is marked by the development of S2 schistosity, which is the main foliation at the outcrop and map-scale with metabasite and orthogneiss bodies parallel to S2 (Figure 1). S2 is marked at mesoscale by (i) leucosome/melanosome alternation in metasedimentary migmatites and in amphibole-bearing ones, (ii) plagioclase- and amphibole-rich layers in banded amphibolites and (iii) garnet porphyroblast orientation and elongation of symplectitic pods in retrogressed eclogites. Scarce evidence of S2 is recognizable in the massive ultrabasic rocks.

S2 strikes from NNW-SSE to NE-SW in the western (Iles locality) and eastern (Nodu Pianu) map areas, respectively. The different orientation of S2 results from large scale folding at the map-scale with development of NW-SE trending hectometre-sized folds (Figure 1), as evidenced by the arcuate shape of the Mt. Nieddu amphibolite lens.

5.2. Metamorphic evolution

The metamorphic evolution of the studied rocks can be schematized as follows:

5.2.1. Migmatite Unit

The metamorphic evolution of migmatites cropping out in the study area has been described by Cruciani et al. (2008a, 2008b; 2014a, 2014b) and Massonne et al. (2013).

The migmatite with trondhjemitic (and minor granitic) leucosomes derived from syn-D1-pre-D2 partial melting of a pelite/psammite sequence in the kyanite stability field. Partial melting was followed by two stages of metamorphic re-equilibration, (i) syn-D2 fibrolite-biotite intergrowth and (ii) post-D2 growth of coarse-grained, late-crosscutting muscovite. An orthogneiss sample from Golfo Aranci yielded a weighted mean $^{40}Ar–^{39}Ar$ white mica age of 304 ± 1.6 Ma, whereas biotite ages are within ∼ 290 −310 Ma (Di Vincenzo et al., 2004).

P-T conditions of partial melting in the neighbouring amphibole-bearing migmatite were ∼1.3 GPa and 700°C (Massonne et al., 2013). Leucosomes crystallized from the melt at P-T conditions close to 1.05 GPa and 700°C with the formation of centimetric amphibole crystals. The complete crystallization of the melt occurred at 0.9 GPa and 680°C. Zircon rim domains in the leucosome of amphibole-bearing migmatite yielded average U-Pb age of 324.2 ± 4.0 Ma, indicating the final stage of partial melting (Cruciani et al., 2019b). The $^{40}Ar–^{39}Ar$ amphibole age of 317.4 ± 2 Ma is related to the time when migmatites were below the P-T conditions of partial melting, i.e. at sub-solidus conditions.

5.2.2. Montigiu Nieddu Unit

The metamorphic evolution of the amphibolite and banded amphibolite cropping out in the study area was reconstructed by Scodina et al. (2019). The garnet-bearing layers (Figure 2(e) and Figure 3(a,b)) recorded the early metamorphic history while the subsequent retrograde equilibration is documented by the host amphibolite. A remarkable increase in pressure (from 0.7 to 1.4 GPa) and a very slight increase in temperature marks their prograde path, reaching maximum pressure conditions in the granulite facies at T = 690–740°C and P = 1.3–1.5 GPa. Afterwards, a decompression with a slight temperature decrease led to the growth of clinopyroxene + plagioclase symplectite, coronae and matrix in the garnet-bearing layers. Subsequently, the amphibolites experienced growth of green amphibole and plagioclase at amphibolite-facies conditions (560–620°C, 0.7–0.8 GPa). Late formation of epidote veins, chlorite and actinolite suggests further retrograde evolution towards the greenschist facies.

Scodina et al. (2020) distinguished three metamorphic stages in the rocks of layer B. The first stage is characterized by the formation of coronitic microstructures of orhopyroxene, clinopyroxene, and garnet developed around igneous olivine and plagioclase (Figure 3(c,d)) and symplectitic (clinopyroxene, spinel) minerals. The second stage corresponds to the pervasive growth of amphibole in the matrix and over the coronitic assemblage, together with the formation of a new spinel generation. Chlorite, talc and corundum also belong to this stage. A third metamorphic stage resulted in the local growth of late phases (i.e.

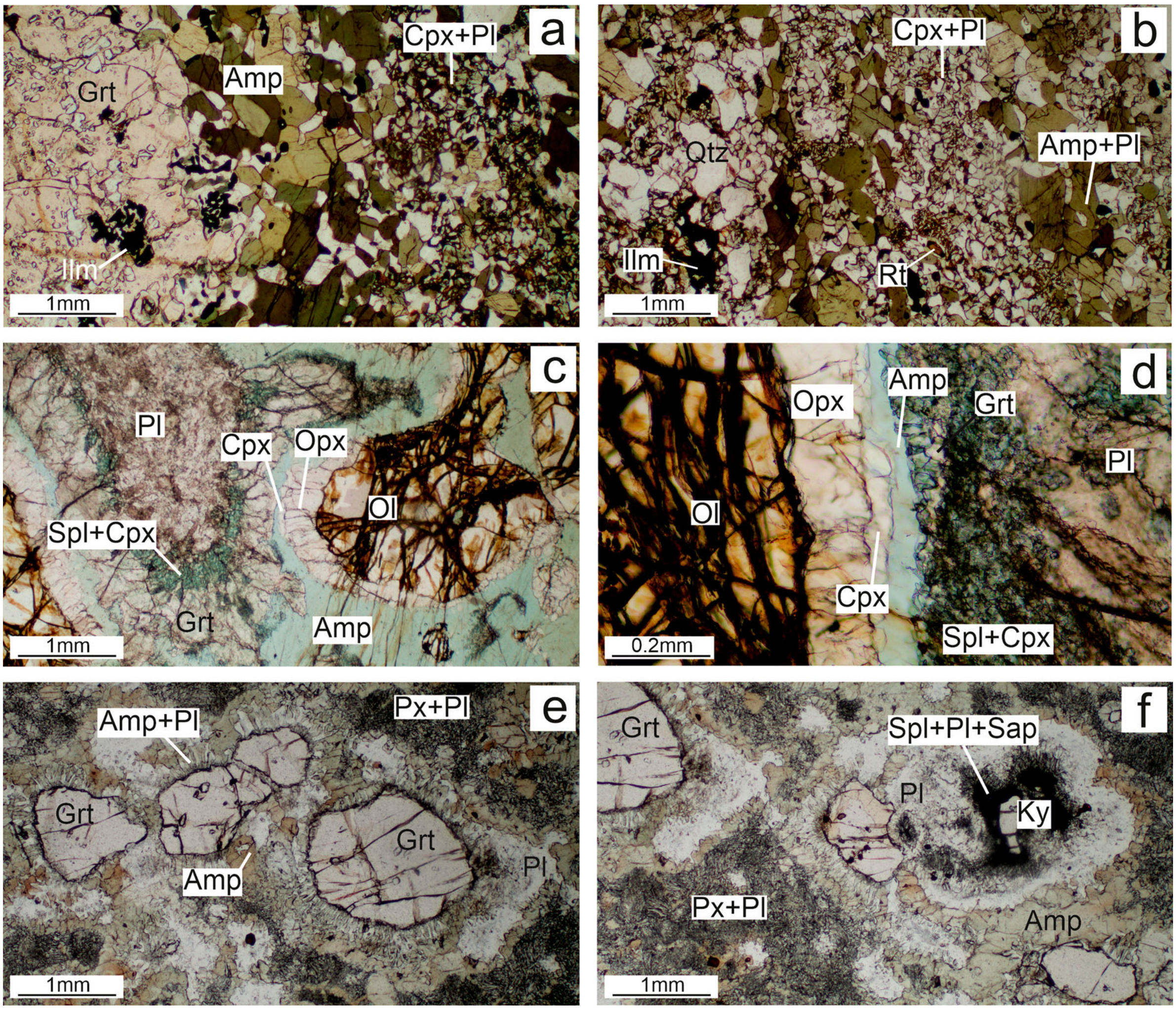

Figure 3. Microphotographs showing the most relevant microstructures of metabasites, plane-polarized light. (a) Garnet porphyroblast and a clinopyroxene + plagioclase symplectite in the garnet-bearing layers of the banded amphibolite. (b) Overview of the matrix of the garnet-bearing layers made of amphibole + plagioclase, quartz, clinopyroxene + plagioclase symplectite, ilmenite and rutile. (c) Coronitic microstructure of pyroxene and garnet around olivine and plagioclase in Layer B of the ultrabasic amphibolite rocks. (d) Detail of the sequence of coronitic minerals. (e) Garnet porphyroblasts and coronitic microstructures of amphibole and plagioclase in the Iles retrogressed eclogite. The garnet crystals are in turn surrounded by symplectite of pyroxene + plagioclase. (f) Kyanite surrounded by spinel + plagioclase and sapphirine + plagioclase symplectites in the Iles retrogressed eclogite. Pl = plagioclase; Ol = olivine; Grt = garnet; Opx = orthopyroxene; Cpx = clinopyroxene; Amp = amphibole; Spl = spinel; Rt = rutile; Ilm = ilmenite; Qtz = quartz; Sap = sapphirine; Ky = kyanite; Px = pyroxene.

actinolite, chlorite, epidote) replacing minerals from the previous stages.

5.2.3. Kyanite-bearing retrogressed eclogite

Kyanite-bearing retrogressed eclogites, cropping out at Iles, experienced a polyphase metamorphic evolution (Cruciani et al., 2019a).

Garnet, kyanite, and omphacite belong to the pre-symplectite stage together with quartz, epidote, apatite, and rutile inclusions preserved in garnet (Figure 3(e)). Eclogite-facies P-T conditions were recorded by garnet compositional zoning.

Plagioclase + clinopyroxene (±orthopyroxene and amphibole) symplectite in the rock matrix, and preserved inside the garnet porphyroblasts, documents a metamorphic stage with development of symplectite minerals (Figure 3(e)). Spinel + anorthite and sapphirine + anorthite symplectites surrounding kyanite porphyroblasts (Figure 3(f)) also developed at this stage, which corresponds to granulite-facies conditions (Giacomini et al., 2005).

The development of plagioclase + amphibole coronitic assemblages at the garnet/symplectite interface, as well as the plagioclase moat that surrounds sapphirine + anorthite symplectite, testifies the occurrence of a corona stage at amphibolite-facies conditions (Giacomini et al., 2005). A post-corona stage at greenschist-facies P-T conditions is documented by the local growth of actinolite, chlorite, and minor epidote and titanite in the rock matrix. In the Golfo Aranci eclogites, Giacomini et al. (2005) determined a U-Pb weighted average age of 352 ± 3 Ma, which is interpreted as the timing of a complete resetting of the U–Pb systematics of zircon. It is difficult to assess whether this age is related to the eclogitic or to the post-eclogitic metamorphic equilibration.

5.3. P-T evolution

The metamorphic P-T conditions and P-T path of the rocks have been reported by Giacomini et al. (2005, 2006), Cruciani et al. (2008a, 2008b, 2014a, 2014b, 2019a), Massonne et al. (2013) and Scodina et al. (2019, 2020).

5.3.1. Migmatite Unit

According to Cruciani et al. (2008a, 2008b, 2014a, 2014b) and Massonne et al. (2013), only the retrograde part of the migmatite P-T trajectory can be reconstructed, since most of its prograde part was overprinted by peak metamorphism.

The migmatite protolith underwent partial melting at HP conditions (T ~ 700–740°C, P ~ 1.1–1.3 GPa) with approximately 1.5–2.0 wt.% H_2O (Cruciani et al., 2014a). Subsequently, pressure release and slight cooling resulted in the crystallization of the leucosome melt to form kyanite and biotite at ~660–730°C, ~0.75–0.90 GPa. After the formation of kyanite-bearing leucosomes, the migmatite underwent metamorphic re-equilibration with the formation of fibrolite and late crosscutting muscovite. The trondhjemitic leucosomes were generated by H_2O-fluxed melting, whereas the rare granitic leucosomes reveal peritectic K-feldspar produced by muscovite-dehydration melting.

The amphibole-bearing migmatite protolith was an intermediate igneous rock. Before partial melting, the H_2O stored in minerals was estimated to be nearly 1.5 wt.% and the free H_2O <1 wt. %. At the P-T conditions of partial melting (1.3 GPa and 700°C), the melt separated from the rock to form leucosomes. Subsequently, pressure decrease accompanied by slight cooling led to the crystallization of the leucosome melt to form large amphibole crystals, that were subsequently partially resorbed. The amphibole resorption probably occurred at 0.9 GPa and 680°C (Massonne et al., 2013). The clockwise P-T path reconstructed by Massonne et al. (2013) implies that the melt must have resided in the rock during exhumation from about 45 to 30 km depth and thus over a long period of time.

5.3.2. Montigiu Nieddu Unit

The dark-green, massive to weakly foliated Mt. Nieddu amphibolite underwent a burial path which was recorded by the compositional zoning of garnet. The P-T path started at pressures of 0.8 GPa and showed only a slight increase in temperature leading to peak P-T conditions. The garnet rim records peak P-T conditions of 1.3–1.4 GPa at 690–740°C. As the early exhumation of the amphibolites occurred already at lower temperatures than the burial, an anticlockwise P-T path results, which is in contrast to the typical clockwise P-T paths reported for several HP metamorphic rocks from NE Sardinia (Scodina et al., 2019).

Rocks with coronitic textures around igneous olivine and plagioclase belonging to the ultrabasic amphibolites of Mt. Nieddu are also characterized by an anticlockwise P-T path (Scodina et al., 2020). Their history starts with the igneous stage at $P < 0.5$ GPa and T = 780–850°C, which was followed by cooling and increasing pressure values until metamorphic P-T conditions of the granulite-facies were reached. At this stage, coronitic microstructures, symplectites, and garnet formed up to 1.3–1.7 GPa and 680–730°C. Exsolution of Fe-oxides from igneous orthopyroxene also occurred at this stage. Subsequently, the rocks underwent a strong retrogression with decompression accompanied by cooling towards the amphibolite- and greenschist-facies.

5.3.3. Kyanite-bearing retrogressed eclogite

The retrogressed eclogites from Iles documented a clockwise P-T path, recorded by the compositional zoning of garnet porphyroblasts and reconstructed by the P-T pseudosection approach by Cruciani et al. (2019a). Estimated conditions are T = 580–630°C and $P = 1.5$–2.0 GPa for the formation of the garnet core, T = 620–690°C and $P = 2.0$–2.3 GPa for the garnet mantle, and T = 650–700°C and $P = 1.4$–2.1 GPa for the growth of the garnet rim.

Giacomini et al. (2005), using conventional thermobarometry, documented for the same rocks a clockwise P-T path very similar to that reported by Cruciani et al. (2019a). The P-T path is similar to that reported in literature for eclogites from nearby localities such as Punta Orvili and Punta de li Tulchi (Cruciani et al., 2011; 2012) and in general for the eclogitic rocks belonging to the Migmatite Complex.

6. Conclusions

Field survey, sampling and structural investigation allowed the production of a 1:10,000 scale geological map of a 7–8 km^2 wide crustal sector belonging to the Variscan Migmatite Complex in the Golfo Aranci area (NE Sardinia), that contributes to the understanding of the evolution of the Variscan orogeny.

In particular, geological mapping has allowed us to pursue the following main goals:

- detailed mapping of lithological units with different metamorphic evolution;
- definition of spatial relation between different metasedimentary and meta-igneous lithological units;
- field reconnaissance of metamorphic mineral assemblages and texture as well as deformation structures.

In summary, in the northern Sardinia Migmatite Complex, all these data allow to document the occurrence of both clockwise and anticlockwise Variscan metamorphic evolution in high-grade metamorphic rock units. In the scenario of late Palaeozoic continental collision, these lithological units derived from lower continental plate (clockwise) and upper continental plate (anticlockwise) and were tectonically joined during the early Carboniferous exhumation stage.

Software

The cartographic database was built using the ArcGIS software, whereas the drawing and layout work were made using the CorelDRAW X5 graphic suite.

Acknowledgements

The authors are grateful to Laura Gaggero, Heike Apps and Hans-Joachim Massonne for their helpful comments.

Disclosure statement

No potential conflict of interest was reported by the author(s).

Funding

Financial support was provided by Regione Autonoma della Sardegna, L.R. 7/2007, research program 'Il blocco Sardo-Corso: area chiave per la ricostruzione della geodinamica varisica' CUP J81G17000110002 and by Fondazione di Sardegna research program 'Geogenic and anthropogenic sources of minerals and elements: fate and persistency over space and time in sediments' CUP F74I19000960007.

References

Carmignani, L., Carosi, R., Di Pisa, A., Gattiglio, M., Musumeci, G., Oggiano, G., & Pertusati, P. C. (1994). The Hercynian chain in Sardinia (Italy). *Geodinamica Acta*, *7*(1), 31–47. https://doi.org/10.1080/09853111.1994.11105257

Carmignani, L., Oggiano, G., Barca, S., Conti, P., Salvadori, I., Eltrudis, A., Funedda, A., & Pasci, S. (2001). Geologia della Sardegna. Note illustrative della Carta Geologica della Sardegna a scala 1:200.000. *Memorie Della Società Geologica Italiana*, *60*, 283.

Carosi, R., Frassi, C., Iacopini, D., & Montomoli, C. (2005). Post collisional transpressive tectonics in northern Sardinia (Italy). *Journal of the Virtual Explorer*, *19*, paper 3. https://doi.org/10.3809/jvirtex.2005.00118

Carosi, R., Montomoli, C., Tiepolo, M., & Frassi, C. (2012). Geochronological constraints on postcollisional shear belt in the Variscides of Sardinia. *Italy. Terra Nova*, *24*(1), 42–51. https://doi.org/10.1111/j.1365-3121.2011.01035.x

Casini, L., Cuccuru, S., Puccini, A., Oggiano, G., & Rossi, P. (2015). Evolution of the Corsica–Sardinia batholith and late-orogenic shearing of the Variscides. *Tectonophysics*, *646*, 65–78. https://doi.org/10.1016/j.tecto.2015.01.017

Corsi, B., & Elter, F. M. (2006). Eo-Variscan (Devonian?) melting in the High-Grade Metamorphic Complex of the NE Sardinia Belt (Italy). *Geodinamica Acta*, *19*(3–4), 155–164. https://doi.org/10.3166/ga.19.155-164

Cruciani, G., Fancello, D., Franceschelli, M., Scodina, M., & Spano, M. E. (2014a). Geothermobarometry of Al-silicate-bearing migmatites from the Variscan chain of NE Sardinia, Italy: A P-T pseudosection approach. *Periodico di Mineralogia*, *83*(1), 19–40. https://doi.org/10.2451/2014PM0002.

Cruciani, G., Franceschelli, M., Elter, F. M., Puxeddu, M., & Utzeri, D. (2008a). Petrogenesis of Al silicate-bearing trondhjemitic migmatites from NE Sardinia, Italy. *Lithos*, *102*(3–4), 554–574. https://doi.org/10.1016/j.lithos.2007.07.023

Cruciani, G., Franceschelli, M., Foley, S. F., & Jacob, D. E. (2014b). Anatectic amphibole and restitic garnet in some Variscan migmatite from NE Sardinia, Italy: Insights into partial melting from mineral trace elements. *European Journal of Mineralogy*, *26*(3), 381–395. https://doi.org/10.1127/0935-1221/2014/0026-2376

Cruciani, G., Franceschelli, M., & Groppo, C. (2011). P-T evolution of eclogite-facies metabasite from NE Sardinia, Italy: Insights into the prograde evolution of Variscan eclogites. *Lithos*, *121*(1-4), 135–150. https://doi.org/10.1016/j.lithos.2010.10.010

Cruciani, G., Franceschelli, M., Groppo, C., Oggiano, G., & Spano, M. E. (2015a). Re-equilibration history and P-T path of eclogites from Variscan Sardinia, Italy: A case study from the medium-grade metamorphic complex. *International Journal of Earth Sciences*, *104*(3), 797–814. https://doi.org/10.1007/s00531-014-1095-5

Cruciani, G., Franceschelli, M., Groppo, C., & Spano, M. E. (2012). Metamorphic evolution of non equilibrated granulitized eclogite from Punta de li Tulchi (Variscan Sardinia) determined through texturally controlled thermodynamic modelling. *Journal of Metamorphic Geology*, *30*(7), 667–685. https://doi.org/10.1111/j.1525-1314.2012.00993.x

Cruciani, G., Franceschelli, M., Jung, S., Puxeddu, M., & Utzeri, D. (2008b). Amphibole-bearing migmatite from Variscan Belt of NE Sardinia, Italy: Partial melting of a mid-Ordovician igneous source. *Lithos*, *102*(3–4), 208–224. https://doi.org/10.1016/j.lithos.2008.03.009

Cruciani, G., Franceschelli, M., Langone, A., & Puxeddu, M. (2019b). U-Pb zircon and Ar-Ar amphibole ages from Sardinian migmatites (Italy) and review of migmatite ages from the Variscan belt. *Periodico di Mineralogia*, *88*, 203–219. https://doi.org/10.2451/2019PM850

Cruciani, G., Franceschelli, M., Langone, A., Puxeddu, M., & Scodina, M. (2015b). Nature and age of pre-Variscan eclogite protoliths from the low- to medium-grade metamorphic complex of north-central Sardinia (Italy) and comparison with coeval Sardinian eclogites in the northern Gondwana context. *Journal of the Geological Society*, *172*(6), 792–807. https://doi.org/10.1144/jgs2015-011

Cruciani, G., Franceschelli, M., Massonne, H.-J., Carosi, R., & Montomoli, C. (2013a). Pressure-temperature and deformational evolution of high pressure metapelites from Variscan NE Sardinia, Italy. *Lithos*, *175–176*, 272–284. https://doi.org/10.1016/j.lithos.2013.05.001

Cruciani, G., Franceschelli, M., Musumeci, G., Spano, M. E., & Tiepolo, M. (2013b). U-Pb zircon dating and nature of metavolcanics and metarkoses from the Monte Grighini Unit: New insights on late Ordovician magmatism in the Variscan Belt in Sardinia, Italy. *International Journal of Earth Sciences*, *102*(8), 2077–2096. https://doi.org/10.1007/s00531-013-0919-z

Cruciani, G., Franceschelli, M., Scodina, M., & Puxeddu, M. (2019a). Garnet zoning in kyanite-bearing eclogite from

Golfo Aranci: New data on the early prograde P-T evolution in NE Sardinia, Italy. *Geological Journal*, *54*(1), 190–205. https://doi.org/10.1002/gj.3169

Cruciani, G., Montomoli, C., Carosi, R., Franceschelli, M., & Puxeddu, M. (2015c). Continental collision from two perspectives: A review of Variscan metamorphism and deformation in northern Sardinia. *Periodico di Mineralogia*, *84*, 657–699. https://doi.org/10.2451/2015PM0455

Di Vincenzo, G., Carrosi, R., & Palmeri, R. (2004). The relationship between tectono-metamorphic evolution and argon isotope records in white mica: Constraints from in situ $^{40}Ar–^{39}Ar$ laser analysis of the Variscan basement of Sardinia. *Journal of Petrology*, *45*(5), 1013–1043. https://doi.org/10.1093/petrology/egh002

Elter, F. M., Padovano, M., & Kraus, R. K. (2010). The emplacement of Variscan HT metamorphic rocks linked to the interaction between Gondwana and Laurussia: Structural constraints in NE Sardinia (Italy). *Terra Nova*, *22*(5), 369–377. https://doi.org/10.1111/j.1365-3121.2010.00959.x

Fancello, D., Cruciani, G., Franceschelli, M., & Massonne, H.-J. (2018). Trondhjemitic leucosomes in paragneisses from NE Sardinia: Geochemistry and P-T conditions of melting and crystallization. *Lithos*, *304–307*, 501–517. https://doi.org/10.1016/j.lithos.2018.02.023

Franceschelli, M., Carcangiu, G., Caredda, A. M., Cruciani, G., Memmi, I., & Zucca, M. (2002). Transformation of cumulate mafic rocks to granulite and re-equilibration in amphibolite and greenschist facies in NE Sardinia, Italy. *Lithos*, *63*(1–2), 1–18. https://doi.org/10.1016/S0024-4937(02)00121-4

Franceschelli, M., Puxeddu, M., & Cruciani, G. (2005). Variscan metamorphism in Sardinia, Italy: Review and discussion. *Journal of the Virtual Explorer*, *19*, paper 2. https://doi.org/10.3809/jvirtex.2005.00121

Franceschelli, M., Puxeddu, M., Cruciani, G., & Utzeri, D. (2007). Metabasites with eclogite facies relics from Variscides in Sardinia, Italy: A review. *International Journal of Earth Sciences*, *96*(5), 795–815. https://doi.org/10.1007/s00531-006-0145-z

Ghezzo, C., Memmi, I., & Ricci, C. A. (1979). Un evento granulitico nel basamento metamorfico della Sardegna nord-orientale. *Memorie Della Società Geologica Italiana*, *20*, 23–38.

Giacomini, F., Bomparola, R. M., & Ghezzo, C. (2005). Petrology and geochronology of metabasites with eclogite facies relics from NE Sardinia: Constraints for the Palaeozoic evolution of Southern Europe. *Lithos*, *82*(1-2), 221–248. https://doi.org/10.1016/j.lithos.2004.12.013

Giacomini, F., Bomparola, R. M., Ghezzo, C., & Guldbransen, H. (2006). The geodynamic evolution of the Southern European Variscides: Constraints from the U/Pb geochronology and geochemistry of the lower Palaeozoic magmatic-sedimentary sequences of Sardinia (Italy). *Contributions to Mineralogy and Petrology*, *152*(1), 19–42. https://doi.org/10.1007/s00410-006-0092-5

Massonne, H.-J., Cruciani, G., & Franceschelli, M. (2013). Geothermobarometry on anatectic melts: A high-pressure Variscan migmatite from NE Sardinia. *International Geology Review*, *55*(12), 1490–1505. https://doi.org/10.1080/00206814.2013.780720

Massonne, H.-J., Cruciani, G., Franceschelli, M., & Musumeci, G. (2018). Anticlockwise pressure–temperature paths record Variscan upper-plate exhumation: Example from micaschists of the Porto Vecchio region, Corsica. *Journal of Metamorphic Geology*, *36*(1), 55–77. https://doi.org/10.1111/jmg.12283

Padovano, M., Dörr, W., Elter, F. M., & Gerdes, A. (2014). The East Variscan Shear Zone: Geochronological constraints from the Capo Ferro area (NE Sardinia. *Italy). Lithos*, *196–197*, 27–41. https://doi.org/10.1016/j.lithos.2014.01.015

Padovano, M., Elter, F. M., Pandeli, E., & Franceschelli, M. (2012). The East Variscan Shear Zone: New insights into its role in the late carboniferous collision in southern Europe. *International Geology Review*, *54*(8), 957–970. https://doi.org/10.1080/00206814.2011.626120

Scodina, M., Cruciani, G., Franceschelli, M., & Massonne, H.-J. (2019). Anticlockwise P-T evolution of amphibolites from NE Sardinia, Italy: Geodynamic implications for the tectonic evolution of the Variscan Corsica-Sardinia block. *Lithos*, *324–325*, 763–775. https://doi.org/10.1016/j.lithos.2018.12.003

Scodina, M., Cruciani, G., Franceschelli, M., & Massonne, H.-J. (2020). Multilayer corona textures in the high-pressure, metaultrabasic rocks of Mt. Nieddu, NE Sardinia (Italy): equilibrium versus disequilibrium. *Periodico di Mineralogia*, *89*(2), online April 2020. https://doi.org/10.2451/2020PM933